Clim Dyn
DOI 10.1007/s00382-011-1154-6

The coherent interdecadal changes of East Asia climate in mid-summer simulated by BCC_AGCM 2.0.1

Haoming Chen · Rucong Yu · Jian Li · Xiaoge Xin · Zaizhi Wang · Tongwen Wu

Received: 20 February 2011 / Accepted: 21 July 2011

Abstract This study proposes primary diagnostic metrics to evaluate the integrated structure of interdecadal changes of East Asian climate in mid-summer (July–August) over the recent half-century (1955–2000) in numerical models. The metrics are applied to comprehensively examine the performance of BCC_AGCM (Beijing Climate Center atmospheric general circulation model) version 2.0.1. When forced by historical sea surface temperatures (SST), the ensemble simulation with the BCC_AGCM reasonably reproduced the coherent interdecadal changes of rainfall, temperature and circulation. The main feature of the "southern-flooding-and-northern-drought" rainfall change is captured by the model. Correspondingly, the tropospheric cooling in the upper and middle troposphere, the southward shift of upper level westerly jet and weakening of the low-level southwesterly monsoon flow are also reproduced, as well as their relationships with rainfall changes. One of the main deficiencies of the simulation is that the amplitudes of the changes of tropospheric cooling and large-scale circulation are both much weaker than those in reanalysis, and they are consistent with the rainfall deficiency. Also, the upper and middle troposphere cooling center and decreasing of upper-level westerly jet axis shift westward in the model simulations compared with that in the observations. Overall, although BCC_AGCM shows problems in simulating the interdecadal changes of East Asia climate, especially the amplitude and locations of change centers, it reasonably represents the observed configuration of rainfall variation and the associated coherent temperature and circulation changes. Therefore, it could be further used to discuss the mechanisms of the interdecadal variation in East Asia. Meanwhile, the reasonably reproduced configuration of rainfall and its associated large-scale circulation by SST-forced runs indicate that the interdecadal variations in East Asia could mostly arise from the regional response to the global climate change.

Keywords Diagnostic metrics · BCC_AGCM · Interdecadal changes · Coherent structure · Model Evaluation

H. Chen · J. Li
Chinese Academy of Meteorological Sciences, China Meteorological Administration, Beijing, China

R. Yu (✉) · X. Xin · Z. Wang · T. Wu
National Climate Center, China Meteorological Administration, No 46 Zhongguancun South Street, Beijing 100081, China
e-mail: yrc@cma.gov.cn

R. Yu
LASG, Institute of Atmospheric Physics, Chinese Academy of Sciences, Beijing, China

J. Li
Dali National Climate Observatory, Dali, China

1 Introduction

The East Asian summer monsoon (EASM) rainfall and circulation over East China have experienced large interdecadal changes during the second half of the 20th century. As a regional response to a decadal shift of atmospheric large-scale circulation in the Northern Hemisphere in the late 1970s (Trenberth and Hurrell 1994), climate changes over the eastern China show distinct three dimensional structures (Yu and Zhou 2007; Yu et al. 2004). A cooling trend in the upper troposphere and lower stratosphere over East Asia has led to the weakening in the northward progression of monsoon winds over this region, which

Published online: 04 August 2011

attributes to the weakening of the low-level southwesterly winds and southward shift of the upper-level jet stream (Wang 2001; Xu et al. 2006). Rainfall over the eastern China also experienced a significant change since the late 1970s, with the Yangtze River (YR) valley becoming wetter and the northern China becoming drier in recent decades, a pattern often referred to as "southern-flooding-and-northern-drought" (SFND) in China (Hu 1997; Hu et al. 2003; Menon et al. 2002; Xu 2001; Yu et al. 2004).

The distinct interdecadal change of East Asia climate provides a key test for evaluating model behaviors, and it is extensively investigated in model simulation by previous studies. Menon et al. (2002) suggested that increased rainfall in the south and drought in the north of China over the past several decades may be related to increased black carbon aerosols based on the experiments using Goddard Institute for Space Studies (GISS) climate model, but the corresponding changes of large-scale circulation are not included in their study. Wang et al. (2008) showed that atmospheric heating induced by the rising Tibetan Plateau temperatures can enhance East Asian subtropical frontal rainfall along the Yangtze River valley, but in their experiments, the changes of large-scale circulation in upper and lower troposphere both exhibited opposite change pattern when compared with observations. Li et al. (2010) analyzed the simulations of the National Center for Atmospheric Research (NCAR) community atmospheric model version 3 (CAM3) and the Geophysical Fluid Dynamics Laboratory (GFDL) atmospheric model version 2.1 (AM2.1). They found that the models forced by observed SST are able to reproduce most of the observed circulation changes associated with the weakening of the EASM since the 1970s, but the rainfall change pattern over East China is not realistically simulated by both of the models. The SST-forcing produces increased summer precipitation over the northern Indian Ocean and the western Pacific Ocean but drying over the land areas northwest of these oceanic areas. Nevertheless, these studies mainly focus on the changes of circulation or only emphasize the variability of rainfall, while few studies comprehensive examine and compare the coherent features of the interdecadal variations in observations and in model simulations.

Understanding the model results requires objective diagnostic metrics. In this study, we propose a comprehensive metric to objectively assess the performance of climate models in simulating the interdecadal changes of East Asian climate, focusing on the coherent changes of rainfall and its large-scale environments. The simulation of Beijing Climate Center atmospheric general circulation model version 2.0.1 (hereafter referred to as BCC_AGCM), forced by historical SST, is then examined to access the SST-induced interdecadal changes in the model.

The rest of the paper is organized as follows. Section 2 provides a brief description of the BCC_AGCM model, datasets and the diagnostic metrics. The performance of BCC_AGCM is then accessed based on the metrics and results are shown in Sect. 3. Section 4 provides concluding remarks and discussion.

2 Model, data and diagnostic metrics

2.1 BCC_AGCM model

The model used in this study is BCC_AGCM version 2.0.1, a global state-of-the-art atmosphere model developed in Beijing Climate Center. It originates from the CAM3 developed by the NCAR. The dynamical core is modified as a reference stratified atmospheric temperature and a reference surface pressure are introduced into the governing equations. The modifications are shown to improve the simulated climate at regional and global scales, especially for temperature and wind (Wu et al. 2008). Several new physical parameterizations have been replaced (Wu et al. 2010). The major modification of the model physics includes a new convection scheme, a dry adiabatic adjustment scheme in which potential temperature is conserved, a modified scheme to calculate the sensible heat and moisture fluxes over the open ocean which takes into account the effect of ocean waves on the latent and sensible heat fluxes, and an empirical equation to compute the snow cover fraction. A detailed description of BCC_AGCM can be found in Wu et al. (2010) and Wu (2011). In this study, the model equations are formulated in a horizontal T42 spectral resolution (approximately 2.8° latitude × 2.8° longitude grid) and a terrain-following hybrid vertical coordinate with 26 levels and a rigid lid at 2.914 hPa.

We examine the SST-induced changes in East Asian climate over a 46-year period (1955–2000) based on a set of atmospheric climate model ensembles forced by observed historical SST data (Rayner et al. 2003; Reynolds et al. 2002). A three-member ensemble of runs was performed to produce a reliable climatology. In these runs, the concentrations of greenhouse gases are held constant at their levels of 1990. In addition, the radiative effects of a climatological aerosol dataset (Collins et al. 2006) are taken into account in the calculation of shortwave fluxes and heating rates. The aerosol dataset includes the monthly mean annual cycle of sulfate, sea salt, carbonaceous, and soil–dust aerosols. Each of the runs was driven by the history of global observed SSTs from January 1950 to December 2000. The first 5-year period is discarded as a spin-up process, and the output of the remaining 46-year simulation is used in the analysis.

2.2 Data

To evaluate the model performance, the following observation/reanalysis datasets are used: (1) geopotential heights, zonal and meridional winds, air temperature, and surface pressure from the National Centers for Environmental Prediction (NCEP)–NCAR reanalysis (referred to as NCEP in the following) during 1955–2000 on a 2.5° × 2.5° grid (Kalnay et al. 1996). The results from ERA40 data are almost the same as NCEP (e.g. Yu and Zhou 2007; Yu et al. 2004) and are not shown. (2) Monthly mean precipitation data at 753 stations in China collected and compiled by National Meteorological Information Centre (NMIC) of the China Meteorological Administration (CMA). To facilitate analysis, the original station data were interpolated onto a 0.5° longitude by 0.5° latitude grid by averaging the station data with weights proportional to the inverse of the squared distance between the center of the grid box and the stations within a radius of one degree. If the distance is less than 0.1 degree, the weight number of the station data will be one (Chang 2003). All the data used covers the periods of 1955–2000, and records in mid-summer (July–August) are analyzed here.

2.3 Metrics for evaluation of the decadal variability

As revealed by Yu and Zhou (2007), the interdecadal changes of mid-summer climate over eastern China show marked three-dimensional coherent structures. To objectively evaluate model performance, not only the interdecadal change of rainfall pattern, but also the changes of corresponding large scale temperature and circulation as well as their coherent three-dimensional structure should be examined. The coherent changes of rainfall and large scale temperature and circulation are regarded as the primary diagnostic metrics to evaluate model performance.

3 The interdecadal change simulated by BCC_AGCM

The performance of BCC_AGCM in simulating East Asian climate is firstly accessed by comparing model results against observations and reanalysis (Fig. 1). By comparing Fig. 1a and b, it can be seen that the ensemble simulation of BCC_AGCM runs captures the two major rain belts in China, with one related to the tropical monsoon trough located around 20°N, and the other extending from the southwestern to northeastern China. The simulated rainfall is much weaker in the two main rain belts, with July–August (JA) mean rainfall amount around 4 mm day^{-1} in the model while over 6 mm day^{-1} in observations. The relatively dry region dominated by the western Pacific subtropical high between the two rain belts is also well

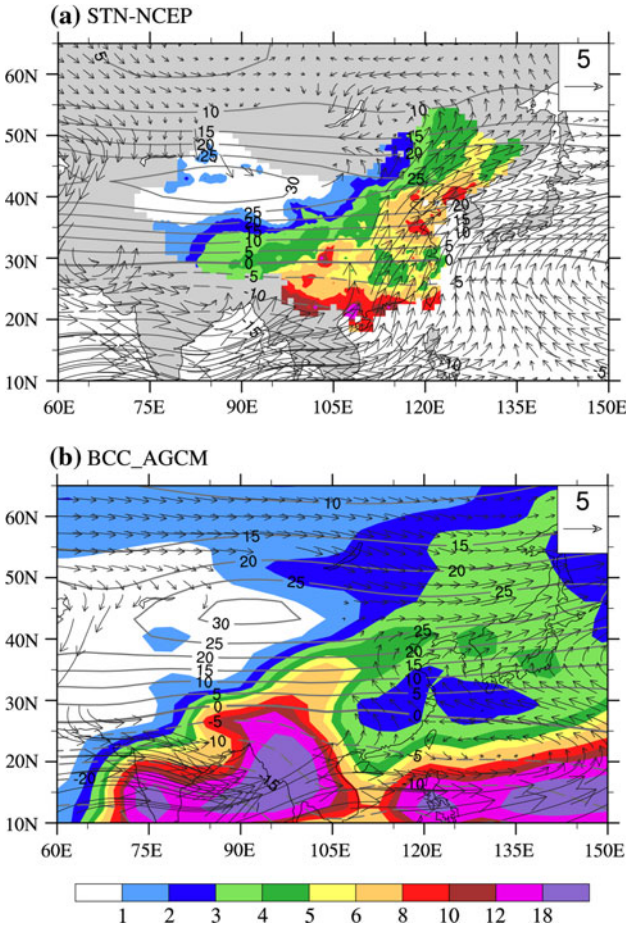

Fig. 1 Mid-summer (July–August) mean precipitation (*shadings*, mm day^{-1}), zonal wind at 200 hPa (*contours*, m s^{-1}) and horizontal wind fields at 850 hPa (*vectors*, m s^{-1}) in **a** station rainfall records and NCEP reanalysis circulation and **b** BCC_AGCM ensemble results

reproduced by the model. The simulated upper troposphere (200 hPa) circulation is comparable to that in NCEP reanalysis data, with the westerly jet axis around 40°N and wind maxima reaching 30 m s^{-1}. In the low-level (850 hPa), the southerly monsoon flow over the south of 40°N is reproduced, but westerly component is much weaker than that in reanalysis data over the eastern China. Meanwhile, westerly prevails in the model, while southwesterly dominates Northeastern China in reanalysis data.

Comparison above shows that BCC_AGCM captures the major climate mean states of East Asian rainfall and large-scale circulation in mid-summer. The interdecadal changes of precipitation are examined in Fig. 2 as precipitation is one of the most important variables used to measure monsoon variability. The spatial distribution of JA rainfall changes (1978–2000 mean minus 1955–1977 mean) are shown in station observation (Fig. 2a) and BCC_AGCM simulation (Fig. 2b) over eastern China. Consistent with the results of previous studies, observed precipitation has increased over the middle and lower reaches of the YR

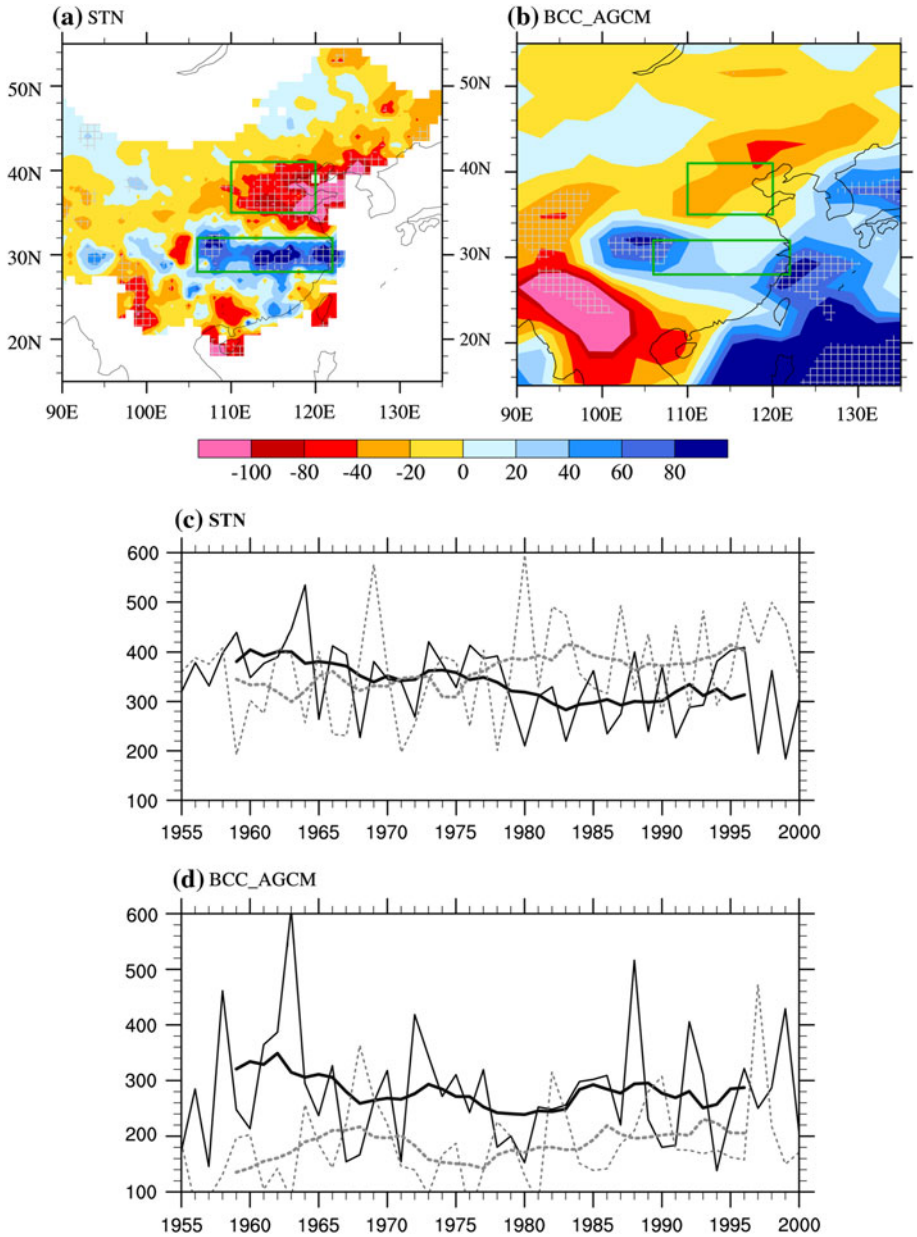

Fig. 2 The 1978–2000 minus 1955–1977 differences of JA (July–August) precipitation (*color shading* unit: mm) from **a** station observations and **b** BCC_AGCM ensemble result. The *gray crosses* indicate where the precipitation change is statistically significant at the 10% level. The *green rectangular boxes* in **a** and **b** show the main observed drought region in North China (north) and flood region in Yangtze River Valley (south). The time series (*thin lines* unit: mm) and 9-year running mean (*thick lines* unit: mm) of JA rainfall **c** observed by stations and **d** simulated by BCC_AGCM are averaged over the south (*gray dotted line*) and north region (*black solid line*) from 1955 to 2000

valley, whereas it has decreased over the northern China. The rainfall anomaly pattern shown in Fig. 2b bears an overall similarity to the observed change pattern, but the amplitude of the change in the model is weaker. A increase of rainfall amount is reproduced along the YR valley, but the flooding center shifts westward to the middle and upper reaches of YR valley (100°E–110°E). The increasing in the lower valley is not significant in the model. The decreasing of rainfall in northern China is much weaker in the model compared to the observation, and it is not statistically significant at the 10% level. Compared with that in former 23 years (1955–1977), the area-averaged JA rainfall amount increases (decreases) by 55.4 mm (66.1 mm) over the south (north) region in observations in latter 23 years (1978–2000), while it increases (decreases) by 35.4 mm (25.6 mm) in model simulation. Meanwhile, a sharp rise of rainfall can be found in the southeastern margin of the Tibetan Plateau, which is also evident in station observations. By comparing Fig. 2b with the results shown by Li et al. (2010), it is found that the BCC_AGCM simulated interdecadal variation of rainfall in eastern China is more reasonable than original CAM3.

In addition to spatial distribution of the differences, the time series of the JA rainfall averaged over the south (106°E–122°E, 28°N–32°N, gray dotted line) and north (110°E–120°E, 35°N–41°N, black solid line) regions are shown in Fig. 2c, d. In observation, the rise in the southern region is consistent during 1955–2000. The decrease in the northern region is evident until the first half of 1980s. A decrease is also found in the last half of the 1990s. The

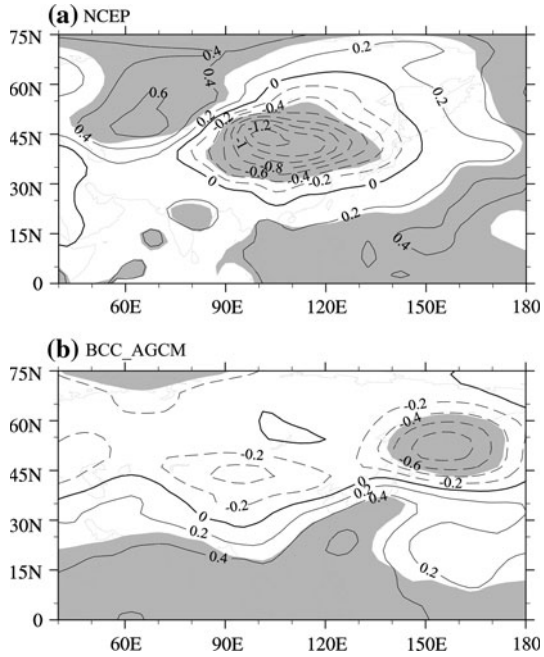

Fig. 3 The 1978–2000 minus 1955–1977 differences of upper and middle level temperature (averaged between 200 and 500 hPa, unit: K) in JA from **a** NCEP reanalysis and **b** BCC_AGCM ensemble result. The *gray shading* indicates where the change is statistically significant at the 10% level

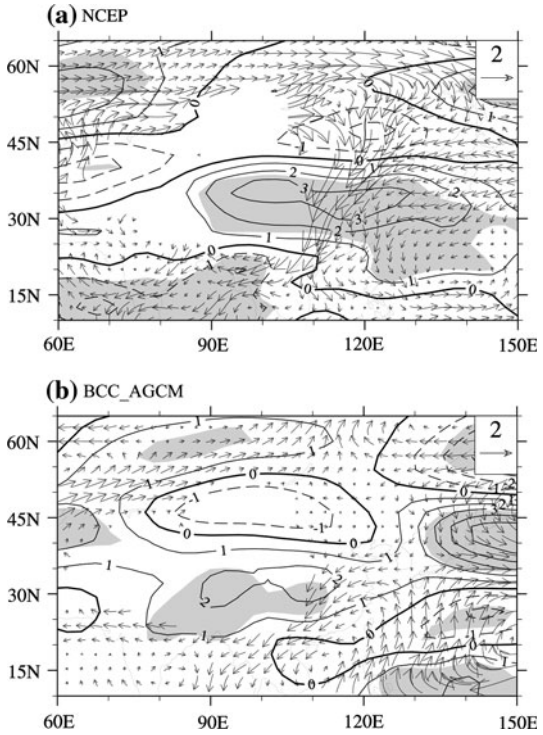

Fig. 4 The 1978–2000 minus 1955–1977 differences of zonal wind at 200 hPa (*contours* unit: m s^{-1}) and wind vectors at 850 hPa (*vectors* unit: m s^{-1}) in JA from **a** NCEP reanalysis and **b** BCC_AGCM ensemble result. The *gray shading* indicates where the change of zonal wind at 200 hPa is statistically significant at the 10% level

correlation between the time series of rainfall in the south and north reaches −0.42 in station observations. The regional mean curves in the model generally resembles that in observation, with the correlation between the two time series in Fig. 2d reaching −0.28. However, the trend is smaller in simulation, consistent with the smaller amplitude of changes as shown in Fig. 2b. The correlation of the averaged rainfall between observation and model simulation is 0.22 in the north and 0.15 in the south, which is partly because the model simulates the wrong location of change centers. In the observed southern flooding region, the simulated increasing rainfall is accompanied by obvious decreasing in 1970s, which causes the less significant change in the model. In the northern drought region, the model simulated the decreasing change, but with an inverse trend in the 1980s. The observed rainfall decreasing from the middle of the 1990s is not obvious in the model.

The interdecadal variability of mid-summer rainfall is closely associated with changes of large scale forcings (Yu and Zhou 2007). A distinctive persistent cooling has occurred in the upper troposphere of East Asia in JA as shown in Fig. 3a. In NCEP reanalysis, the region of significant cooling in JA mean temperature averaged between 200 and 500 hPa covers a large area between 30°N and 45°N and from 90°E to 130°E. The cooling center locates in the northeast of the Tibetan Plateau and exceeds 1 K. To examine the reproduction of this cooling in BCC_AGCM, the change of middle and upper troposphere temperature in the model is shown in Fig. 3b. The BCC_AGCM captures the unique upper troposphere cooling in mid-summer, and the mid-latitude of Eurasia continent is dominated by cooling in the model. The significant cooling region shifts eastward to the northwestern Pacific, reaching approximate 0.6 K. The simulated cooling over the northeast of the Tibetan Plateau, which is less than 0.4 K, is much weaker compared with reanalysis data.

Accompanying with the upper tropospheric cooling, large-scale circulation in mid-summer has also experienced significant changes in East Asia. In the upper troposphere, the westerly jet axis is located around 40°N at 200 hPa (Fig. 1a), which is closely related to the major rain-producing system known as Meiyu front in summer located along the YR valley extending to northwestern Pacific (Tao et al. 1958; Zhang et al. 2006). In the NCEP reanalysis, a notable increase in westerlies (larger than 3 m s^{-1}) is found around 30°N and the decrease of westerly occurs along 45°N (Fig. 4a). As such, the 200 hPa westerly jet over East Asia displaces southward, well corresponding to the "southern-flooding-and-northern-drought" rainfall pattern in eastern China. The BCC_AGCM well simulates the change of upper-level westerly jet (Fig. 4b). The

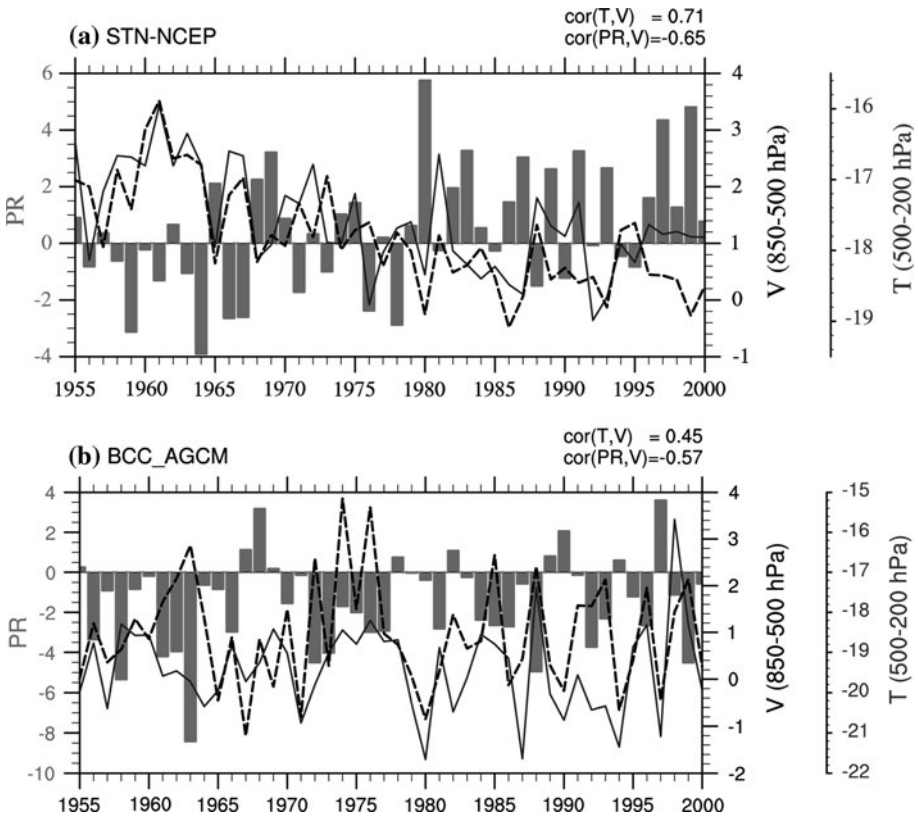

Fig. 5 Time series of the JA mean rainfall rate difference (*gray bars* unit: mm day^{-1}) between the Yangtze River valley (the *south rectangular box* in Fig. 2) and the North China (the *north rectangular box* in Fig. 2), the lower tropospheric (850–500 hPa) southerlies (*black solid line* unit: m s^{-1}) averaged over (105°E–120°E, 30°N–40°N) and the upper tropospheric (500–200 hPa) air temperature (*black dashed line* unit: K) averaged over (90°E–120°E, 30°N–45°N) from **a** station observation and NCEP reanalysis and **b** BCC_AGCM ensemble result

westerly increases 2 m s^{-1} along 30°N and decrease about 1 m s^{-1} along 45°N. Nevertheless, the increasing and decreasing centers shift westward in the model, which is well correlated to the rainfall variation pattern, as the simulated flooding centers along the YR valley is more evident in the region west of 110°E.

Despite the evident changes in the upper troposphere, the low-level monsoon flows also show obvious variation. The interdecadal changes of JA 850 hPa winds from reanalysis and model simulation are compared by vectors in Fig. 4. Summer monsoon flow from Southwest China to Northeast China weakened substantially, as anomalous northerly winds dominate most of East Asia (Fig. 4a). The southwesterly monsoon flows over East China transport water vapor all the way to North China (Zhou and Yu 2005). With the anomalous northerly winds, the actual northward transport of tropical water vapor to North China has reduced while more water vapor converges over the YR valley, corresponding to excessive rainfall in the South and deficient rainfall in the North. The model generally captures the changes of the 850 hPa winds over East Asia, with the weakening of the EASM well reproduced. However, the simulated 850 hPa wind changes are not as large as those in the reanalysis. The northeasterly anomaly mainly locates around region south of 40°N. The weak change of low-level wind in North China is closely related to the bias of climate mean state, since westerly rather than southwesterly prevails the region north of 40°N in the model (Fig. 1b). It is also noted that the weakening of monsoon in BCC_AGCM simulation is even weaker than that in original CAM3 with the same forcing as shown by Li et al. (2010).

From the analyses above, it is found that although BCC_AGCM show problems in simulating the interdecadal changes of East Asia climate, such as the amplitude and location of change centers, the observed configuration of the changes between rainfall and related large scale temperature and circulation is reasonable reproduced by the model. To quantitatively examine the capability of BCC_AGCM in reproducing the relationship of interdecadal changes of upper troposphere cooling and low-level wind weakening, the regional mean time series of low-level meridional wind (averaged over 850–500 hPa) and upper level temperature (500–200 hPa) are illustrated in Fig. 5. The JA mean rainfall difference between the YR valley and North China is also shown. A high correlation between the lower tropospheric meridional wind averaged in 100°E–120°E, 30°N–40°N and the upper-tropospheric air temperature averaged in 90°E–120°E, 35°N–45°N is found in reanalysis (Fig. 5a), with the correlation coefficient reaching 0.71. This weakening of monsoon flow contributes to the interdecadal change of rainfall in the eastern China, and they are highly correlated with each other. The correlation between the low-level southerly and changes of rainfall difference between YR valley and northern China reaches −0.65. The model

reproduces the relationship between the upper-level temperature and low-level meridional wind, as well as that between low-level wind and rainfall difference (Fig. 5b). In most of years, the low-level southerly shows consistent variation with upper-level temperature, while opposite trend with rainfall differences. The correlation between low-level southerly and upper-level temperature is 0.45, smaller than that in reanalysis, partly because the cooling in the upper troposphere and weakening of low-level monsoon circulation in the model is both weaker than those in reanalysis. The negative correlation between low-level southerly and rainfall differences is also well reproduced by the model, with the correlation coefficient reaching −0.57.

To further examine the vertical structure of the changes in temperature and winds, Fig. 6 compares the cross section of zonal mean (90°E–120°E) temperature (contours) and wind vectors from NCEP and BCC_AGCM. Consistent with previous studies, there is a significant cooling over the subtropical (north of 25°N) and a warming over the tropical region (south of 25°N) during 1978–2000 relative to 1955–1977. The cooling center reaches −1.5 K and is around the 300 hPa level over 30°N–50°N. Accompanying this cooling and its resulted change in land–ocean temperature gradients, anomalous descending and ascending motions occur over North China and YR valley, respectively, with anomalous northerly winds prevailing between 20°N and 50°N. The tropospheric cooling in subtropical and warming in the tropical region is captured by the model, with the latter more significant in the simulation (Fig. 6b). The subtropical cooling (about 0.3 K) is much weaker in the model. The cold anomaly shifts southward with the descent of height, locating over the north of YR valley in the middle and lower levels (beneath 400 hPa) while over the North China in the upper levels (above 300 hPa), indicating a baroclinic structure in troposphere in the model. Corresponding to the troposphere cooling, the model reproduces the descending and ascending motions over the tropical ocean area and YR valley, respectively, with anomalous northerly winds between 20°N and 40°N. Consistent with the southward shift of middle and low level cooling, the descending motion shifts southward, and the region north of 40°N is dominated by upward motion and southerly, which coincides with the weak interdecadal variation of rainfall over North China (Fig. 2b).

The meridional mean cross section in changes of temperature and wind averaged over 30°N–45°N is shown in Fig. 7. Significant tropospheric cooling is found from the

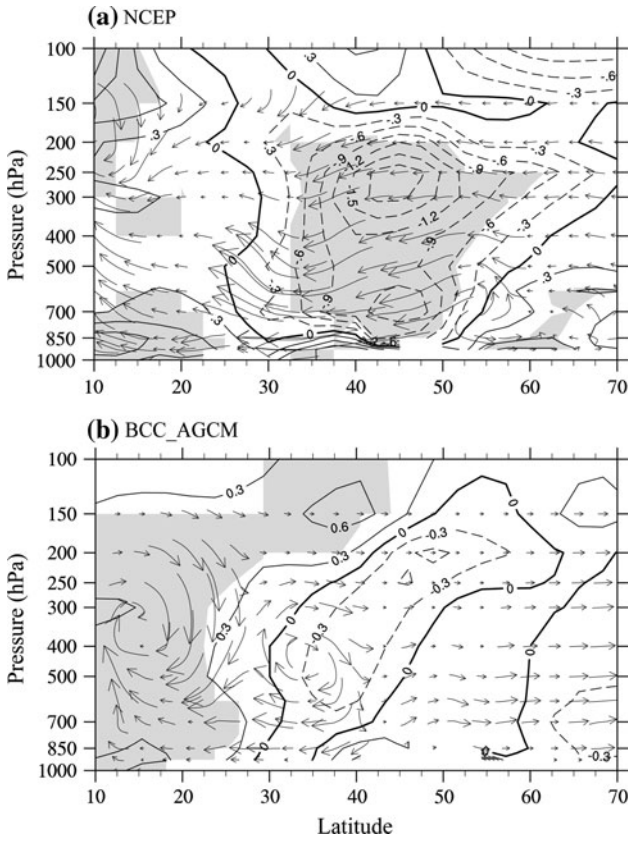

Fig. 6 Mean latitude-height cross section averaged over 90°E–120°E of JA temperature (*contours* unit: K) and meridional circulation (*vectors*) for 1978–2000 minus 1955–1977 difference from **a** NCEP reanalysis and **b** BCC_AGCM ensemble result. The *shaded areas* in are statistically significant at the 10% level for temperature

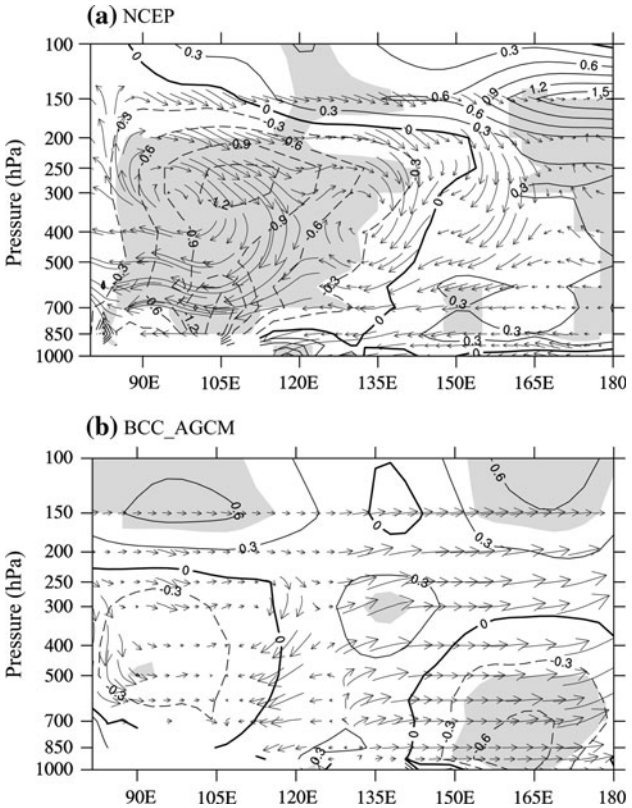

Fig. 7 Same as Fig. 6, but for mean longitude-height cross section averaged over 30°N–45°N

Tibetan Plateau to the eastern China (80°E–130°E). The cooling center is also at 300 hPa around 105°E in reanalysis data (Fig. 7a). A relative weaker warming is found over the region west of 75°E and east of 150°E. Corresponding to the changes of tropospheric temperature, strong downward motion is found over the eastern China. The westerly over the upper troposphere (above 300 hPa) of the eastern China increases, while easterly over the lower levels (below 400 hPa) increases, indicating the enhancement of subtropical westerly jet in upper troposphere and weakening of southwesterly monsoon wind in low levels. The broad zonal vertical structure is also captured by the model (Fig. 7b). The troposphere cooling in the model mainly situates upon the Tibetan Plateau (90°E–105°E) below 300 hPa, about 20° westward compared with the reanalysis. The spatial range of cooling is much smaller and the amplitude is much weaker. Increased westerly in upper troposphere is also reproduced, while the decrease of low-level westerly is only evident around 105°E–120°E.

4 Conclusion remarks and discussion

4.1 Conclusions

To comprehensive examine the interdecadal changes of East Asian climate in second half of the 20th century, the rainfall change and its related three-dimensional structure of temperature and circulation as a whole are proposed as primary metrics to access the performance of BCC_AGCM. The SST-induced changes simulated by a set of ensemble runs show that the BCC_AGCM captures the observed configuration of the interdecadal changes of East Asian climate in mid-summer. The main results are summarized below.

1. The "southern-flooding-and-northern-drought" rainfall pattern is generally simulated by the model. However, the center of rainfall change is not well reproduced. The flooding center in the south shifts westward. Meanwhile, the amplitude of the change, especially in the north, is much weaker compared to the observation.
2. The tropospheric cooling, southward shift of upper level westerly jet and weakening of low-level monsoon flow are all reasonably captured. The amplitudes of these changes are all smaller than that in reanalysis and the change centers shift.
3. Although the model still exhibits large biases, the configuration of the observed changes of rainfall and its associated large-scale temperature and circulation is faithfully reproduced by the model.

4.2 Discussion

Simulations of the Asian summer monsoon and its variability are challenging issues due to the complex of the associated physical processes (Kang et al. 2002; Wang et al. 2005; Gao et al. 2011). In this study, we proposed the configuration of rainfall and its related three dimensional structures of tropospheric cooling and associated circulation as a primary metric to comprehensively examine model results. Several other factors also greatly influence the EASM and its variability. For example, the western Pacific subtropical high (WPSH) is one of the most important and direct factor. Previous investigations have shown that zonal and meridional location of WPSH are directly and closely associated with the interdecadal variations of EASM. The southwesterly monsoon flow is largely affected by WPSH (Tao and Chen 1987; Huang et al. 2003; Liu et al. 2004; Ding and Chan 2005; Zhou and Yu 2005; Zhou et al. 2009). In addition, Indian Ocean and tropical eastern Pacific (ENSO) may also have contribution to the interdecadal variations (Hu 1997; Liang et al. 2009).

Studying how East Asian climate have changed may provide insight for understanding future changes. Numerical models are useful tool to study the mechanism of East Asian climate. Building comprehensive metrics for evaluating key model behaviors and understanding critical processes should help to improve model performance and further help to understand the contribution of different factors to EASM and its variability. By comparing the results of BCC_AGCM with observation and reanalysis data using the primary diagnostic metric, this study lays down a base for further investigation of the physical processes associated with the interdecadal variations of East Asian summer climate by using GCM. It is suggested that although there are systematical biases in current version of BCC_AGCM, this model reasonably captures the observed configuration of coherent temperature and circulation changes, as well as their relationships with rainfall changes. Therefore, this model has implications for the interpretation of mechanisms of the interdecadal changes in the East Asia.

We have used a prescribed SST boundary condition in this study. The reasonably reproduced configuration of rainfall and related large-scale circulation in the SST-forced runs support the perspective that the interdecadal changes of East Asian rainfall and circulation are mainly a regional response to global climate changes rather than regional anthropogenic forcing agents. Nevertheless, it should be noted that the observed SST includes both natural variability and response to anthropogenic forcing such as increasing of GHG concentrations, the reproduction of East Asian summer monsoon interdecadal variation in the GCM forced by observed SST cannot exclude the impact

of increase of GHG concentration on the decadal variation of East Asian summer monsoon. Our conclusion does not rule out any other factors. To better understand the roles of other forcing agents including aerosols, future studies are needed by coupling BCC_AGCM with an ocean model. However, whether the coupled model is possible to correctly simulate the long term trend of summer monsoon rainfall over this region warrants further study.

Acknowledgments We thank the anonymous reviewers for their helpful detailed comments. This work was jointly supported by the Major National Basic Research Program of China on Global Change under Grant 2010CB951902 and the National Natural Science Foundation of China under Grants 40625014 and 40921003.

References

Chang K-T (2003) Introduction to geographic information systems (in Chinese), 2nd edn. Science Press, Moscow, pp 245–254

Collins WD, Rasch PJ, Boville BA, Hack JJ, McCaa JR, Williamson DL, Briegleb BP, Bitz CM, Lin S-J, Zhang M (2006) The formulation and atmospheric simulation of the community atmosphere model version 3 (CAM3). J Clim 19:2144–2161. doi:10.1175/JCLI3760.1

Ding Y, Chan JCL (2005) The East Asian summer monsoon: an overview. Meteorol Atmos Phys 89:117–142

Gao H, Yang S, Kumar A, Hu Z–Z, Huang B, Li Y, Jha B (2011) Variations of the East Asian Mei-Yu and simulation and prediction by the NCEP climate forecast system. J Clim 24:94–108

Hu Z–Z (1997) Interdecadal variability of summer climate over East Asia and its association with 500 hPa height and global sea surface temperature. J Geophys Res 102:19403–19412. doi:10.1029/97jd01052

Hu Z–Z, Yang S, Wu R (2003) Long-term climate variations in China and global warming signals. J Geophys Res 108:4614. doi:10.1029/2003jd003651

Huang R, Zhou L, Chen W (2003) The progresses of recent studies on the variabilities of the East Asian monsoon and their causes. Adv Atmos Sci 20:55–69

Kalnay E, Kanamitsu M, Kistler R, Collins W, Deaven D, Gandin L, Iredell M, Saha S, White G, Woollen J, Zhu Y, Chelliah M, Ebisuzaki W, Higgins W, Janowiak J, Mo KC, Ropelewski C, Wang J, Leetmaa A, Reynolds R, Jenne R, Joseph D (1996) The NCEP/NCAR 40-year reanalysis project. Bull Am Meteorol Soc 77:437–471

Kang IS et al (2002) Intercomparison of the climatological variations of Asian summer monsoon precipitation simulated by 10 GCMs. Clim Dyn 19:383–395

Li H, Dai A, Zhou T, Lu J (2010) Responses of East Asian summer monsoon to historical SST and atmospheric forcing during 1950–2000. Clim Dyn 34:501–514. doi:10.1007/s00382-008-0482-7

Liang J, Yang S, Hu Z–Z, Huang B, Kumar A, Zhang Z (2009) Predictable patterns of the Asian and Indo-Pacific summer precipitation in the NCEP CFS. Clim Dyn 32:989–1001

Liu Y, Wu G, Ren R (2004) Relationship between the subtropical anticyclone and diabatic heating. J Clim 17:682–698

Menon S, Hansen J, Nazarenko L, Luo Y (2002) Climate effects of black carbon aerosols in China and India. Science 297:2250–2253. doi:10.1126/science.1075159

Rayner NA, Parker DE, Horton EB, Folland CK, Alexander LV, Rowell DP, Kent EC, Kaplan A (2003) Global analyses of sea surface temperature, sea ice, and night marine air temperature since the late nineteenth century. J Geophys Res 108:4407. doi:10.1029/2002jd002670

Reynolds R, Rayner N, Smith T, Stokes D, Wang W (2002) An improved in situ and satellite SST analysis for climate. J Clim 15:1609–1625

Tao S, Chen L (1987) A review of recent research on the East Asian summer monsoon in China. In: Chang CP, Krishnamurti TN (eds) Monsoon meteorology. University Press, Oxford

Tao S, Zhao Y, Chen X (1958) The association between Mei-Yu in East Asia and seasonal variation of the general circulation of atmosphere over Asia (In Chinese). Acta Meteorologica Sinica 29:119–134

Trenberth KE, Hurrell JW (1994) Decadal atmosphere-ocean variations in the Pacific. Clim Dyn 9:303–319. doi:10.1007/bf00204745

Wang H (2001) The weakening of the Asian monsoon circulation after the end of 1970's. Adv Atmos Sci 18:376–386. doi:10.1007/bf02919316

Wang B, Ding Q, Fu X, Kang I-S, Jin K, Shukla J, Doblas-Reyes F (2005) Fundamental challenge in simulation and prediction of summer monsoon rainfall. Geophys Res Lett 32:L15711. doi:10.1029/2005GL022734

Wang B, Bao Q, Hoskins B, Wu G, Liu Y (2008) Tibetan Plateau warming and precipitation changes in East Asia. Geophys Res Lett 35:L14702. doi:10.1029/2008gl034330

Wu T (2011) A mass-flux cumulus parameterization scheme for large-scale models: description and test with observations. Clim Dyn. doi:10.1007/s00382-011-0995-3

Wu T, Yu R, Zhang F (2008) A modified dynamic framework for the atmospheric spectral model and its application. J Atmos Sci 65:2235–2253. doi:10.1175/2007JAS2514.1

Wu T, Yu R, Zhang F, Wang Z, Dong M, Wang L, Jin X, Chen D, Li L (2010) The Beijing Climate Center atmospheric general circulation model: description and its performance for the present-day climate. Clim Dyn 34:123–147. doi:10.1007/s00382-008-0487-2

Xu Q (2001) Abrupt change of the mid-summer climate in central east China by the influence of atmospheric pollution. Atmos Environ 35:5029–5040. doi:10.1016/s1352-2310(01)00315-6

Xu M, Chang C-P, Fu C, Qi Y, Robock A, Robinson D, Zhang H-M (2006) Steady decline of East Asian monsoon winds, 1969–2000: evidence from direct ground measurements of wind speed. J Geophys Res 111:D24111. doi:10.1029/2006jd007337

Yu R, Zhou T (2007) Seasonality and three-dimensional structure of interdecadal change in the East Asian monsoon. J Clim 20:5344–5355

Yu R, Wang B, Zhou T (2004) Tropospheric cooling and summer monsoon weakening trend over East Asia. Geophys Res Lett 31:L22212. doi:10.1029/2004gl021270

Zhang Y, Kuang X, Guo W, Zhou T (2006) Seasonal evolution of the upper-tropospheric westerly jet core over East Asia. Geophys Res Lett 33:L11708. doi:11710.11029/12006GL026377

Zhou T, Yu R (2005) Atmospheric water vapor transport associated with typical anomalous summer rainfall patterns in China. J Geophys Res 110:D08104. doi:08110.01029/02004JD005413

Zhou T, Yu R, Zhang J, Drange H, Cassou C, Deser C, Hodson DLR, Sanchez-Gomez E, Li J, Keenlyside N, Xin X, Okumura Y (2009) Why the Western Pacific subtropical high has extended westward since the late 1970s. J Clim 22:2199–2215